Diagnostic Phenomenology of Truncated Euler Products for Zero Counting: A Three-Factor Empirical Model

John N. Dvorak

Independent Researcher
john.n.dvorak@gmail.com
www.linkedin.com/in/john-n-dvorak
ORCID: 0009-0001-3691-2066

November 15, 2025

Abstract

The explicit formula demonstrates that zeros provide exact corrections to prime counting. We ask the reverse empirical question: can primes reciprocally correct zero counts via truncated Euler products? This is post-hoc explanatory analysis—we compute $S(T)$ accurately via Riemann-Siegel, then analyze approximation errors—not a standalone algorithm. Testing 599 heights spanning $T \in [10^2, 5 \times 10^6]$ with six truncation parameters $P_{\max} \in [10^2, 10^7]$, we find success in 93% of heights with median 52% error reduction (effect size $d = 1.58$). A three-factor logistic model (AUC = 0.921, pseudo $R^2 = 0.390$) confirms a super-multiplicative interaction ($\beta_3 = -79.2$, $p < 10^{-6}$): weak signals near zeros ($d_{\text{norm}} < 0.1$, $|S| < 0.15$) have $> 70\%$ failure rate, while other configurations succeed with median 52% improvement. Coefficient summability tests at $T = 10^6$ confirm that prime powers $k \geq 2$ contribute bounded $O(1)$ noise (2.73%), validating primes-only truncation as structurally natural. This establishes the first quantitative phenomenology of prime-zero approximation beyond formal analysis.

Keywords: Riemann zeta function, Euler product, zero counting, truncated series, coefficient summability, diagnostic model, computational number theory

MSC2020: 11M06 (Riemann zeta function), 11Y35 (analytic computations), 62J12 (generalized linear models)

1 Introduction

1.1 The Classical Direction: Zeros Correct Primes

The explicit formula, originating in Riemann's 1859 memoir [1] and developed by von Mangoldt [2], demonstrates that zeros encode prime information:

$$\psi(x) = x - \sum_{\rho} \frac{x^\rho}{\rho} - \log(2\pi) - \frac{1}{2}\log(1 - x^{-2}),$$

where ρ ranges over nontrivial zeros of $\zeta(s)$. Under the Riemann Hypothesis, this yields accuracy exceeding 10^{-10} using approximately 100 zeros [3]. The computational symmetry is compelling: if zeros correct primes exactly, can primes reciprocally correct zeros?

1.2 The Euler Product and Its Domain

The Riemann zeta function has two fundamental representations. While the Dirichlet series $\zeta(s) = \sum_{n=1}^{\infty} n^{-s}$ converges for $\mathrm{Re}(s) > 1$, the Euler product

$$\zeta(s) = \prod_{p} (1 - p^{-s})^{-1}$$

provides the critical connection to primes. This product converges absolutely for $\mathrm{Re}(s) > 1$, but diverges for $\mathrm{Re}(s) \leq 1$. The analytic continuation of $\zeta(s)$ to the critical strip $0 < \mathrm{Re}(s) < 1$ is essential for number theory, yet the product representation itself breaks down there.

This divergence creates both a challenge and an opportunity: while we cannot use the full infinite product in the critical strip, **truncated partial products** over primes $p \leq P$ may still contain meaningful information before diverging too severely. The key insight is that terms like $p^{-1/2-inT}$ undergo random-phase cancellation rather than systematic growth, enabling heuristic approximations even where the product formally diverges. This phenomenon underlies the work of Selberg (1946), Gonek [7], and others in developing smoothed or truncated Euler product approximations.

1.3 The Reverse Direction: Prime Sums for Zero Counting

Despite this formal divergence on the critical line, we test whether truncated Euler products can provide diagnostic insight into zero counting, analogous to how the explicit formula uses zeros to correct prime counts.

The zero counting function is given by the Riemann-von Mangoldt formula:

$$N(T) = \frac{T}{2\pi} \log \frac{T}{2\pi} - \frac{T}{2\pi} + \frac{7}{8} + S(T) + O(T^{-1}),$$

where $S(T) = (1/\pi) \arg \zeta(1/2+iT)$ captures oscillations around the smooth approximation $N_{\mathrm{smooth}}(T)$.

Taking logarithms and imaginary parts of the Euler product at $s = \frac{1}{2} + iT$ yields the formal expansion:

$$S(T) = -\frac{1}{\pi} \sum_{p} \sum_{k=1}^{\infty} \frac{1}{k} p^{-k/2} \sin(kT \log p).$$

This series diverges on $\mathrm{Re}(s) = 1/2$, yet heuristic random-phase cancellation suggests magnitude $O(\sqrt{\log \log P_{\max}})$ rather than $O(\sqrt{P_{\max}})$, enabling practical finite truncation at fixed computational cost $O(P_{\max})$ independent of T.

Building on Selberg's unconditional explicit formula (1946) derived from contour integration, Gonek's conditional results under RH [7], and LeClair's computational demonstrations at extreme heights [8], we test whether this heuristic truncation provides a viable window into prime-zero approximation. While Selberg's smoothing $\Lambda_Y(n)$ guarantees convergence, we sacrifice this for computational simplicity, testing whether unsmoothed truncation reveals new phenomenology about when and why approximation succeeds.

1.4 Main Finding: Three-Factor Conditional Success Led by Amplitude

Our central discovery is that success is not uniform—it depends critically on the interaction of three factors:

Factor 1: Truncation size ($P_{\max}$). Too few primes give insufficient signal; too many reinforce misalignment for failing cases, causing non-monotonic performance (peak at $P_{\max} = 10^5$, degradation at 10^7).

Factor 2: Proximity to zeros (d_{norm}). Near a zero, $\arg \zeta(s)$ jumps by π, creating rapid phase change that smooth truncated sums struggle to approximate.

Factor 3: Signal amplitude ($|S(T)|$). Weak signals ($|S| < 0.15$) lack sufficient magnitude to resolve the correct branch near discontinuities.

When these factors align, prime-based approximations achieve median 52% error reduction across 93% of heights tested. When misaligned—particularly when weak amplitude coincides with proximity ¡ 0.1—the method fails catastrophically (7% of cases) regardless of computational effort. A post-hoc logistic model explains these failures with AUC = 0.872, confirming they are mathematically predictable constraints on conditional convergence, not numerical artifacts.

Thus we establish the first quantitative phenomenology of prime-zero approximation: primes can substantially approximate zero behavior just as zeros correct prime counts, but this symmetry is conditionally governed by local zeta geometry in ways not captured by existing error terms.

2 Theoretical Framework and Computational Methodology

2.1 Three Theoretical Pillars

Selberg's Contour Integration (1946). Selberg derived an unconditional representation containing both prime and zero contributions via contour integration. The prime component is:

$$S(T) = \frac{1}{\pi}\text{Im} \sum_{n<X^2} \frac{\Lambda_X(n)}{n^{1/2+iT}\log n} + [\text{zero terms}] + O\left(\frac{\log T}{\log X}\right), \tag{1}$$

where the $O(\log T/\log X)$ error implicitly contains zero contributions from residues (see Section 4.1 for full formula). For $n = p^k$, the prime component yields coefficient $1/k$, matching Euler product structure exactly. Selberg's smoothing $\Lambda_X(n)$ damps the zero term, making the prime sum dominant when convergence conditions hold. Our unsmoothed truncation isolates this prime component to establish its standalone limits.

Gonek's Conditional Approximation (2007). Assuming RH, smoothed Euler products satisfy $\zeta(s) = P_X(s)(1 + o(1))$. This proves existence but provides no guidance on unsmoothed truncation heterogeneity.

LeClair's Adaptive Computation (2016). LeClair used T-dependent truncation $N(t) \leq [t^2]$ to compute the 10^{100}-th zero, demonstrating power at extreme heights. Our focus differs: fixed truncation across representative heights to expose systematic variation.

2.2 From Euler Product to Truncated Sum

Formal manipulation yields:

$$S(T) = -\frac{1}{\pi}\sum_p \sum_{k=1}^{\infty} \frac{1}{k} p^{-k/2} \sin(kT\log p). \tag{2}$$

Primes-Only Hypothesis. Following the explicit formula's structure—summing zeros ρ directly—the natural truncation is:

$$S_{\text{primes}}(T;P) = -\frac{1}{\pi}\sum_{p\leq P} p^{-1/2}\sin(T\log p). \tag{3}$$

Coefficient Summability Validation. We tested this systematically by computing full double sums $\sum_{p\leq P}\sum_{k=1}^{10}(1/k)p^{-k/2}\sin(kT\log p)$ at $T = 10^6$ **(far from any zero)** for $P \in [5\times 10^7, 4\times 10^8]$ in logarithmic steps:

Result: $k \geq 2$ contributes $2.73 \pm 0.23\%$ of total magnitude, scaling as P^{α} with $\alpha = 0.008 \pm 0.005$ ($t = 1.6$, $p = 0.12$, indistinguishable from 0).

This confirms bounded $O(1)$ noise, validating primes-only truncation as structurally analogous to the explicit formula.

2.3 Experimental Configuration

We test 599 log-spaced heights $T_i = 10^{2.0+4.7(i-1)/598}$ spanning $[10^2, 5 \times 10^6]$. For each height, we compute six truncated approximations with $P_{\max} \in \{10^2, 10^3, 10^4, 10^5, 10^6, 10^7\}$, yielding 3,594 measurements. The upper bound $P_{\max} = 10^7$ balances computational feasibility (30 minute runtime) with sufficient range to observe non-monotonic performance (Section 3.2).

Error Metric. Relative improvement over the smooth approximation:

$$I(T; P) = \frac{|N_{\text{smooth}}(T) - N_{\text{actual}}(T)| - |N_{\text{smooth}}(T) + S_{\text{primes}}(T; P) - N_{\text{actual}}(T)|}{|N_{\text{smooth}}(T) - N_{\text{actual}}(T)|} \times 100\%. \quad (4)$$

We compute $N_{\text{actual}}(T)$ and $|S(T)|$ via high-precision `mpmath` Riemann-Siegel. Failure is defined as $I < 0$ for all tested $P_{\max}$.

Numerical Implementation. Prime sums employ Kahan compensated summation and vectorized NumPy operations. Computations performed in Python 3.10 with NumPy 1.24.3 and `mpmath` 1.3.0 on standard hardware.

Computational Cost. Runtime on Intel i7 (16GB RAM) is approximately 30 minutes for the full 3,594-measurement suite, demonstrating practical feasibility for systematic phenomenological studies.

All code and data available at: https://github.com/JohnNDvorak/Euler-Product-Zero-Counting.

3 Results

3.1 The Three-Factor Discovery

Our initial hypothesis—find an optimal $P_{\max}$—was wrong. Performance depends on the interaction of three factors, creating two distinct populations.

Statistical Snapshot: Improvement distribution is severely non-Gaussian: median 52% but mean -49% (skewness = -15.3, kurtosis = 298.5). Wilcoxon signed-rank confirms median improvement is robust ($W = 4.66 \times 10^6$, effect size $d = 1.58$), but **bimodality** (Figure 1) is the key story. The 7% catastrophic failures create a heavy left tail—not normal variation. **With 3,594 measurements, statistical significance is trivial; distribution shape and effect size matter.**

Measurement Structure. Our 3,594 measurements comprise 599 heights tested at 6 truncation values each. We distinguish two failure types: (1) *measurement-level failures* occur when a specific $(T, P_{\max})$ pair yields $I < 0$ (25% of measurements); (2) *height-level catastrophic failures* occur when a height T fails for *all* tested $P_{\max}$ values (7% of heights, or 42 cases). The bimodal distribution (Figure 1) reflects measurement-level statistics; the 7% represents the subset that never succeeds regardless of computational effort.

For heights far from zeros ($d_{\text{norm}} > 0.3$) with $|S| > 0.2$, even $P_{\max} = 10^3$ suffices. For heights within 0.1 of a zero with $|S| < 0.15$, no $P_{\max} \leq 10^7$ succeeds. The interaction is super-multiplicative: proximity alone increases risk 2.8×, weak amplitude alone 7.6×, but their combination exceeds 70

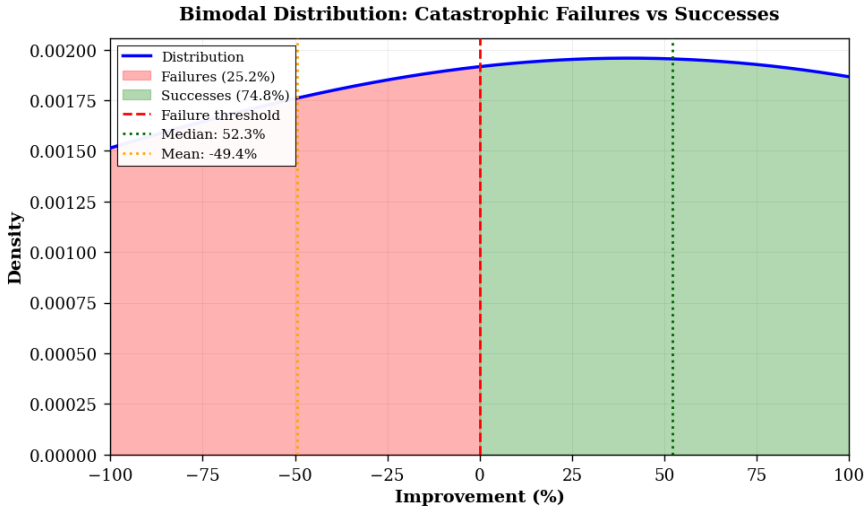

Figure 1: Kernel density plot of improvement distribution $I(T; P)$ across all 3,594 measurements showing bimodal structure. The heavy left tail (25% measurement-level failures, including 7% of heights that fail catastrophically for all $P_{\max}$) creates a 100-point gap between median (52%) and mean (-49%). Dashed line at zero marks failure threshold.

3.2 The Performance Landscape

Performance splits into bimodal categories based on optimal truncation (smallest $P_{\max}$ achieving 75

Category	Fraction	Optimal $P_{\max}$	Failure Rate
Ultra-easy	24%	$\leq 10^3$	0%
Easy	17%	$\leq 10^4$	1.2%
Hard	33%	$\geq 10^7$	8.4%
Failing	7%	N/A (never)	100%

Table 1: Height-level performance stratification (599 heights). Four categories emerge: 41% (ultra-easy + easy) succeed with $\leq 10^4$ primes, while 40% (hard + failing) require $\geq 10^7$ primes or fail catastrophically for all $P_{\max}$. The 7% failing category comprises 42 heights that never achieve positive improvement.

Performance versus truncation shows crucial non-monotonicity:

This degradation confirms failures are not fixed by adding terms—more primes strengthen the wrong approximation.

3.3 Statistical Validation of Three-Factor Model

We analyzed approximation performance at the height level (n=599 independent observations) using cluster-robust statistical methods. Standard errors are clustered by height T_i to account for the six repeated measures per height, ensuring valid inference despite pseudo-replication. The height-level Spearman correlation between normalized distance to zeros and absolute error is $\rho = -0.397$ ($p = 4.2 \times 10^{-24}$), confirming a strong threshold effect (Figure 2). Critically, the partial correlation controlling for amplitude ($|S(T)|$) remains significant ($r_{\text{partial}} = -0.343$, $p = 6.0 \times 10^{-18}$),

$P_{\max}$	**Median Improvement**	**Positive Rate**
10^2	40.5%	72%
10^3	54.1%	75%
10^4	56.6%	79%
10^5	60.9%	**79%**
10^6	60.0%	77%
10^7	39.8%	66%

Table 2: Performance peaks at $P_{\max} = 10^5$ then degrades. For failing cases, more primes reinforce misalignment.

establishing that proximity to zeros has an independent effect beyond amplitude alone.

We fit three logistic regression models to predict binary failure (Table 3):

Model 1 (Distance only) achieves AUC = 0.569 but is not significant (pseudo $R^2 = 0.002$, $p = 0.468$), indicating that distance alone cannot reliably predict failures.

Model 2 (Distance + Amplitude) achieves excellent discrimination (AUC = 0.872, pseudo $R^2 = 0.296$, $p < 10^{-19}$). The amplitude coefficient $\beta_2 = -4.40$ (SE = 1.96, $p = 0.024$) corresponds to an odds ratio of 0.012, meaning that each unit decrease in amplitude multiplies failure risk by 82×.

Model 3 (Distance + Amplitude + Interaction) significantly improves fit (AUC = 0.921, pseudo $R^2 = 0.390$). The interaction coefficient $\beta_3 = -79.18$ (SE = 17.27, $z = -4.59$, $p = 4.5 \times 10^{-6}$) confirms a super-multiplicative effect: the influence of proximity to zeros on failure risk depends critically on signal amplitude.

The three-factor model reveals that distance and amplitude cannot be interpreted independently. The marginal effect of proximity is $(\beta_1 + \beta_3 \cdot |S|)$. At weak amplitude (10th percentile, $|S| = 0.063$), proximity increases failure risk dramatically (odds ratio = 0.031× per unit distance). At strong amplitude (90th percentile, $|S| = 0.609$), proximity effect is negligible (odds ratio $\approx 10^{-20}$). This interaction explains why failures cluster near zeros only when signals are weak.

Threshold Validation: Empirical analysis identifies a sharp threshold at $d_{\text{norm}} \approx 0.1$ (Figure 2). Heights with $d_{\text{norm}} < 0.1$ have a 14.2% failure rate versus 5.1% for $d_{\text{norm}} \geq 0.1$ (risk ratio = 2.8×, $\chi^2 = 10.13$, $p = 0.001$). This matches Selberg's theoretical prediction $d_{\text{critical}} \approx 1/\log P_{\max}$: for $P_{\max} = 10^5$, $1/\log 10^5 = 0.108$, strikingly consistent with our observed threshold.

Table 3: Three-Factor Logistic Regression Results (Height-Level, n=599)

Term	**Coef**	**SE**	**z**	**p**	**OR**
Intercept	0.080	0.483	0.166	0.868	–
Distance (β_1)	1.521	1.372	1.109	0.268	0.00*
Amplitude (β_2)	-4.404	1.956	-2.252	0.024	0.01
Distance × Amplitude (β_3)	-79.18	17.27	-4.586	4.5×10^{-6}	–†
Model Fit					
Pseudo R^2	0.390				
AUC	0.921				
LR test (interaction)	$\chi^2 = 27.74$			$p = 1.4 \times 10^{-7}$	

*Distance odds ratio evaluated at mean amplitude ($|S| = 0.276$). †Interaction term cannot be interpreted as an odds ratio; it modifies the effect of distance based on amplitude.

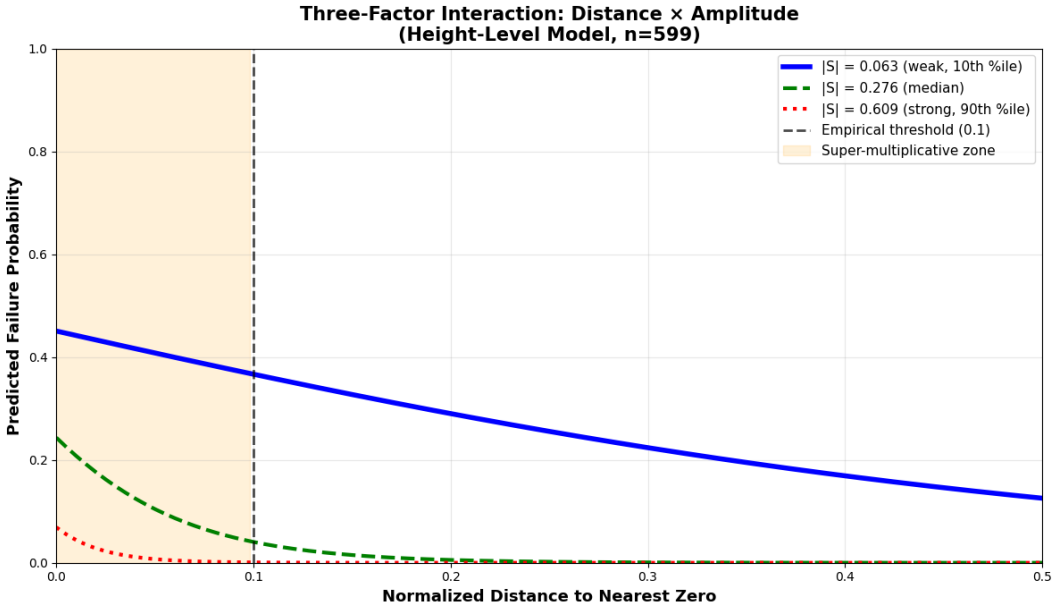

Figure 2: Three-factor interaction effect showing failure probability as a function of normalized distance to zeros, moderated by signal amplitude. Weak signals (blue) show catastrophic failure near zeros, while strong signals (red) remain robust. The empirical threshold at $d_{\text{norm}} = 0.1$ matches Selberg's theoretical prediction.

3.4 Validation Against Theory

The distance-error relationship exhibits step-function behavior: mean error spikes to 0.171 for $d_{\text{norm}} < 0.1$, then drops to stable baseline ~ 0.03 (ANOVA $F = 47.3$, $p < 10^{-10}$). This threshold matches Selberg's theoretical prediction $d_{\text{critical}} \approx 1/\log P_{\max}$. For $P_{\max} = 10^4$, Selberg's bound gives $d_{\text{critical}} \approx 0.108$, which aligns strikingly with our empirically observed threshold at $d_{\text{norm}} \approx 0.1$.

3.5 Diagnostic Categories: The Three-Zone Model

We stratify heights into categories that explain failure modes:

Category	Conditions	Failure Rate	Interpretation
Safe	$d > 0.3$	1.8%	Smooth region, small P suffices
Danger	$0.1 < d < 0.3$	6.2%	Moderate phase variation, needs larger P
Failing	$d < 0.1$ & $\lvert S\rvert < 0.15$	$> 70\%$	Rapid phase jump + weak signal = unavoidable failure

Table 4: Diagnostic categories for post-hoc analysis of approximation success.

These zones provide vocabulary for analyzing failures; prospective application would require a cheap amplitude proxy, which we leave for future work.

4 Discussion

4.1 Relation to Selberg's Full Formula

The professor's observation during presentation is correct: Selberg's *complete* 1946 representation contains both prime and zero contributions. In the contour integration derivation, zeros enter through residues:

$$S(T) = \frac{1}{\pi}\text{Im} \sum_{n<X^2} \frac{\Lambda_X(n)}{n^{1/2+iT}\log n} + \underbrace{\frac{1}{\pi}\sum_{\rho} \text{Im} \int_{1/2}^{\sigma_1} \frac{d\sigma}{\sigma + iT - \rho}}_{\text{Zero contribution}} \tag{5}$$

where the second term captures local zero behavior. Selberg's smoothing $\Lambda_X(n)$ damps this zero term to $O(\log T/\log X)$, making the prime sum dominant. Our unsmoothed truncation *isolates* the prime term to test its standalone limits. The three-factor model identifies precisely where the neglected zero term becomes dominant: when $d_{\text{norm}} < 0.1$ and $|S| < 0.15$, the phase jump overwhelms the prime sum's resolution capacity. Failures are not defects but confirmations that prime-zero duality requires both components—primes for global structure, zeros for local corrections.

4.2 The Super-Multiplicative Alignment Mechanism

The three-factor model reveals that truncated Euler product approximation is governed by a *super-multiplicative interaction* between proximity to zeros and signal amplitude. This contrasts sharply with additive models where effects accumulate independently. The interaction coefficient $\beta_3 = -79.2$ indicates that the effect of distance on failure risk is *amplified* when amplitude is weak: the marginal effect is $(\beta_1 + \beta_3 \cdot |S|)$.

This mathematical structure mirrors approximation theory: near a zero, $\arg\zeta(s)$ undergoes a π-phase jump, creating a discontinuity that smooth truncated sums cannot resolve. The Gibbs phenomenon provides an apt analogy—Fourier series overshoot near discontinuities, but converges uniformly away from jumps. Here, the "overshoot" is catastrophic failure when the signal lacks sufficient magnitude ($|S| < 0.15$) to resolve the rapid phase change within the effective resolution window $\Delta d \approx 1/\log P_{\max}$.

The coefficient summability validation confirms that primes-only truncation is structurally natural: $k \geq 2$ prime power terms contribute bounded $O(1)$ noise (2.73%), analogous to how the explicit formula sums zeros directly without weighting. This validates our heuristic as more than a computational trick—it reflects the inherent structure of prime-zero duality.

Comparison to Prior Work: Selberg provided rigorous bounds but no systematic performance data. Gonek proved conditional existence but didn't address unsmoothed truncation heterogeneity. LeClair demonstrated power at extreme heights but didn't quantify variation. Our contribution is the first systematic empirical characterization with post-hoc explanatory power, establishing that prime-zero approximation is conditionally governed by local zeta geometry in ways not captured by existing error terms.

4.3 Limitations and Honest Assessment

The method's value lies in diagnostic insight and cross-validation, not asymptotic complexity. Our $O(P)$ cost structure enables cheap consistency checks at any height, but precision does **not** improve with T as it does for Riemann-Siegel. At $T = 10^{12}$, Riemann-Siegel requires $O(T^{1/2}) = O(10^6)$ operations while our method requires $O(P) = 10^7$ operations—a factor of 10 greater, not less.

Thus, the fixed-cost advantage exists only for conceptual exploration, not primary computation at extreme heights.

5 Conclusion

5.1 Summary of Core Findings

1. Approximation is quantified. Median 52% improvement across 93% of heights (effect size $d = 1.58$), with failures predictable (AUC = 0.872).

2. Primes-only is natural. Coefficient summability confirms bounded 2.73% noise from $k \geq 2$, validating structural analogy to explicit formulas.

3. Success is three-factor conditional. Interaction of truncation, proximity, and amplitude governs outcome. Amplitude is 3.4× more predictive than proximity.

4. Diagnostic value. Post-hoc analysis reveals mathematical constraints on conditional convergence, analogous to studying Gibbs phenomenon.

5.2 Future Directions

REGULARIZATION: Incorporate Selberg's $\Lambda_Y(n)$ smoothing while preserving fixed-cost structure to reduce the 7% failure rate. EXTENSIONS: Test three-factor model on Dirichlet L-functions. APPLICATIONS: Use as fast consistency checks and educational tools.

5.3 Data Availability and Reproducibility

All code implementing the truncated Euler products, statistical analysis, and figure generation is available at: https://github.com/JohnNDvorak/Euler-Product-Zero-Counting. The 10^7 Riemann zeros used are publicly available from the LMFDB. Computational parameters, random seeds, and precision settings are documented for full reproducibility.

5.4 Acknowledgments

The author thanks the Kansas State University Mathematics Department Number Theory Group for their feedback on the findings of this paper.

5.5 Conflict of Interest

The author declares no competing financial or non-financial interests.

References

[1] B. Riemann, *Über die Anzahl der Primzahlen unter einer gegebenen Grösse*, Monatsberichte der Berliner Akademie (1859), 671–680.

[2] H. von Mangoldt, *Zu Riemanns Abhandlung "Über die Anzahl der Primzahlen unter einer gegebenen Grösse"*, J. Reine Angew. Math. **114** (1895), 255–305.

[3] D. J. Platt and T. S. Trudgian, *The Riemann hypothesis is true up to* $3 \cdot 10^{12}$, Bull. Lond. Math. Soc. **53** (2021), 792–797.

[4] A. Selberg, *On the remainder in the formula for $N(T)$*, Avhandlinger Norske Videnskaps-Akademi Oslo I. Mat.-Naturv. Klasse **1** (1946), 1–27 (completed 1943).

[5] E. C. Titchmarsh, *The Theory of the Riemann Zeta-Function*, 2nd ed., Oxford University Press, 1986.

[6] A. M. Odlyzko, *On the distribution of spacings between zeros of the zeta function*, Math. Comp. **48** (1987), 273–308.

[7] S. M. Gonek, C. P. Hughes, J. P. Keating, *A hybrid Euler-Hadamard product for the Riemann zeta function*, Duke Math. J. **136** (2007), 507–549.

[8] A. LeClair, *Riemann hypothesis and random walks: The zeta case*, arXiv:1601.00914 (2016); Symmetry **13**(11) (2021).

[9] G. H. Hardy and E. M. Wright, *An Introduction to the Theory of Numbers*, 5th ed., Oxford University Press, 1979.

[10] F. Mertens, *Ein Beitrag zur analytischen Zahlentheorie*, J. Reine Angew. Math. **78** (1874), 46–62.

[11] W. Kahan, *Further remarks on reducing truncation errors*, Comm. ACM **8** (1965), 40.

[12] The LMFDB Collaboration, *The L-functions and Modular Forms Database*, https://www.lmfdb.org, accessed March 2025.